EVALUATION OF THE GLOBAL CLOUD COVER PARAMETERS OBTAINED FROM GEOSTATIONNARY DATA IN THE FRAME OF THEMEGHA-TROPIQUES MISSION WITH CALIPSO LIDAR OBSERVATIONS

Geneviève Sèze[1], Hervé Legleau[2], Marcel Derrien[2], Bruno Six[3] and Jacques Pelon[4]

1 LMD/IPSL, Paris, France Email: genevieve.seze@lmd.jussieu.fr
2 Météo-France, Centre de Météorologie Spatiale, Lannion
3 ICARE, UMS 2877, Université de Lille-1
4 LATMOS/IPSL , Paris, France

Abstract

For the need of the MEGHA-Tropique space mission, a coherent cloud mask and cloud type classification is required in the latidudinal band between 40°N and 40°S with a good spatial and temporal sampling. The data from the available geostationary satellites allowing such an approach will be analysed using the retrieval method developed by the SAFNWC for SEVIRI. Cloud and aerosol layer structure observed with CALIOP space base lidar will be used to evaluate and inter-compare these fields. It will be also refered to the ISCCP analysis of the geostationary satellite data. As a first step in this evaluation study, the SEVIRI cloud classification and cloud top pressure have been compared with lidar data. Results are presented for two periods using two different space based lidar data, GLAS lidar data and CALIOP lidar data. Day and night, land and ocean are studied separately.

1. INTRODUCTION

For understanding tropical meteorological and climatic processes, reliable statistics on the water and energy budget of the tropical atmosphere and description of the evolution of its systems (monsoons, cyclones,...) at appropriate time scales are required. The MEGHA-TROPIQUES (MT) mission aims to measure with a high receptivity radiances linked to radiative fluxes, water vapour and precipitation (http://meghatropiques.ipsl.polytechnique.fr). The 20 degree orbit at 870km of altitude allows up to six observations by day of the same region. On board MT, it will be a MW imager for rain and clouds (MADRAS), a MW sounder for water vapour (SAPHIR) and a wide band instrument for radiative fluxes (ScaraB).The geostationary satellite VIS and IR imagers will complete this set of instruments. From these data, cloud mask, cloud type classification and cloud top pressure products over the whole tropical belt (45°S -45°N) will be built each half hour with a spatial resolution of the order of 5kmx5km. These fundamental cloud products will be used as input in the non precipitating cloud algorithm and in the tracking of convective systems. They will bring useful complementary information in the validation step of the radiative budget and fluxes product and the rain estimation. Combined to the other MT measurements, they will allow to analyse the diurnal and life cycle of the cloud cover

During the MT experiment, data from at least five geostationary satellites (MSG, GOES-E, GOES-W, MTSAT, FY-2C for fall 2009) will be collected and analysed using the retrieval method developed by the SAFNWC (Legleau and Derrien, 2005; Derrien and Legleau, 2009). From the geostationary satellite data, cloud mask, cloud type classification and cloud top pressure products over the whole tropical belt (45°S -45°N) will be built at least each hour with a spatial resolution of the order of 5km by 5km using the retrieval method developed by the SAFNWC for SEVIRI. Cloud and aerosol layer structure observed with the lidar CALIOP on board the CALIPSO platform belonging to the AQUA-train satellite constellation will be used to evaluate and inter-compare these fields. The ISCCP geostationary satellite cloud cover will be also used. (Rossow et al. 1999).

As a first step in this evaluation study, the comparison of the SEVIRI cloud classification with space base lidar data has been performed. Results of this evaluation are presented here. Two periods are studied. The first in October 2003 corresponds to the period for which data from the GLAS space base lidar on board the ICESAT platform are available and are of good quality. The second is in October 2006 after the launch of the lidar CALIOP. Day and night, land and ocean are studied separately. In section 2, the geostationary data set and the cloud classification SAFNWC retrieval are presented. In section 3, we introduce the lidar data set, the ISCCP data, the periods and the region used to performed the SEVIRI cloud cover evaluation. In section 4, results are presented. Day and night, land and ocean are studied separately. Conclusions are given in section 5.

2. THE GEOSTATIONARY DATA SET AND THE CLOUD CLASSIFICATION SAFNWC RETRIEVAL

The cloud detection, cloud classification and cloud top pressure retrieval developed by the SAFNWC for SEVIRI (Legleau and Derrien, 2005; Derrien and Legleau, 2009) has been adapted to GOES-E, GOES-W, GOES-10, MTSAT, FY-2C. This set of data which is collected at SATMOS (http://www.satmos.meteo.fr/) and processed at the ICARE data center *(http://www.icare.univ-lille1.fr)* allow to cover all the tropical belt (fig. 1) with a spatial resolution of the order of few kilometers and a repeat cycle of one hour. It has the mandatory channels allowing to apply the SAFNWC algorithm, I.e. one visible channel, two IR channels (10.8µ, 3.9µ), one WV or CO2 sounder channel (table 1). In the futur, this configuration will be adapted as a fonction of the geostationary data sets available.

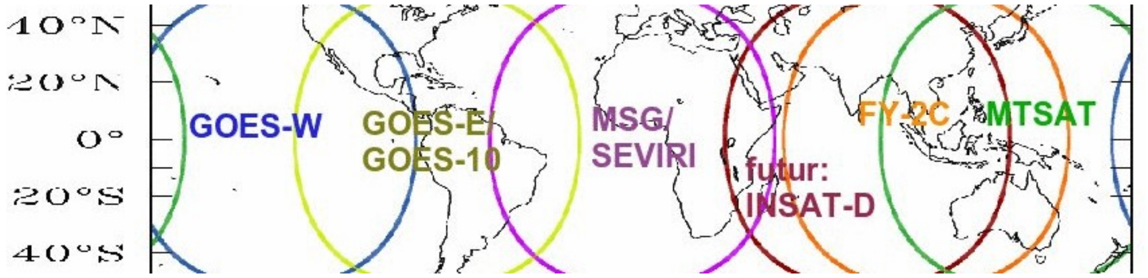

Figure 1: Field of view of the five geostationary satellites plus the futur Indian satellite INSAT-D.

	GOES-W	GOES-E	SEVIRI/MSG	FY-2C	MTSAT
Satellite longitude	135W	75W	3.3W	104.5E	140W
Resolution (IR)	4km	4km	3km	5km	4km
Repeat cycle	G: 1h – NH 30'	G: 1h – NH 30'	G 15'	1h	G: 1h NH 30'
VIS channels	0.6µ, 0.8µ	0.6µ	0.6µ , 0.8µ	0.77µ	0.725µ
IR channels	3.9µ,10.8µ,12.µ	3.9µ,10.8µ	3.9µ,10.8µ,12.µ	3.75µ,10.8µ,12.µ	3.75µ,10.8µ,12.µ
Sounder channels	6.7µ	6.5µ, 13.4µ	6.2µ, 7.3µ, 13.4µ	6.95µ	6.75µ

Table 1: Main characteristics of the GOES-W, GOES-E, SEVIRI/MSG, FY-2C and MTSAT radiometer.

The cloud detection and cloud classification, the two first steps of the SAFNWC algorithm, rely on multi-spectral thresholds tests applied at the pixel scale to a set of spectral and textural features. After sorting between cloud free and cloud contaminated pixels, cloudy pixels are classified in two sets: (1) fractional cloud and elevated semitransparent cloud, (2) low, medium and high thick clouds. Using the same technique, a separation between fractional, high semitransparent cloud (single layer) and high semitransparent in a multi-layered cloud system is performed. For thick and multi-layered clouds the separation in low, middle and high cloud is performed using ancillary temperature and humidity profiles. At the end of the classification process, ten cloud classes are defined, which have here been condensed into six classes : clear, partial, low, middle, high and “cirrus over”. The last class is representative of multilayered systems with cirrus clouds at the upper level. This class is available only for daytime analysis. For opaque clouds, the cloud top height (CTH) is retrieved from the 10.8 µm brightness temperature. For low/middle clouds, tests are applied tending to place the cloud top level below an existing temperature inversion. For high thin clouds, a correction for semi-transparency is applied using two IR channels, a window channel and a sounding one (13.4 , 7.3 or 6.2 µm) as in Schmetz, 1993; Menzel, 1983. For multi-layered situations or pixels partially covered by low clouds no pressure is available.

The SAFNWC algorithm required as ancillary input, surface height maps, land/sea mask, climatological maps of SST, continental reflectance maps, temperature and humidity profils. Thresholds are tuned to radiometer's spectral characteristics with RadiativeTransfer Models in cloud free conditions (6S,RTTOV). All these parameters have been adapted to the GOES-E, GOES-W, GOES-10, FY-2C and MTSAT. Figure 2 give an example of cloud classification obtained for GOES-W, GOES-E, SEVIRI and MTSAT for day data and for night data.

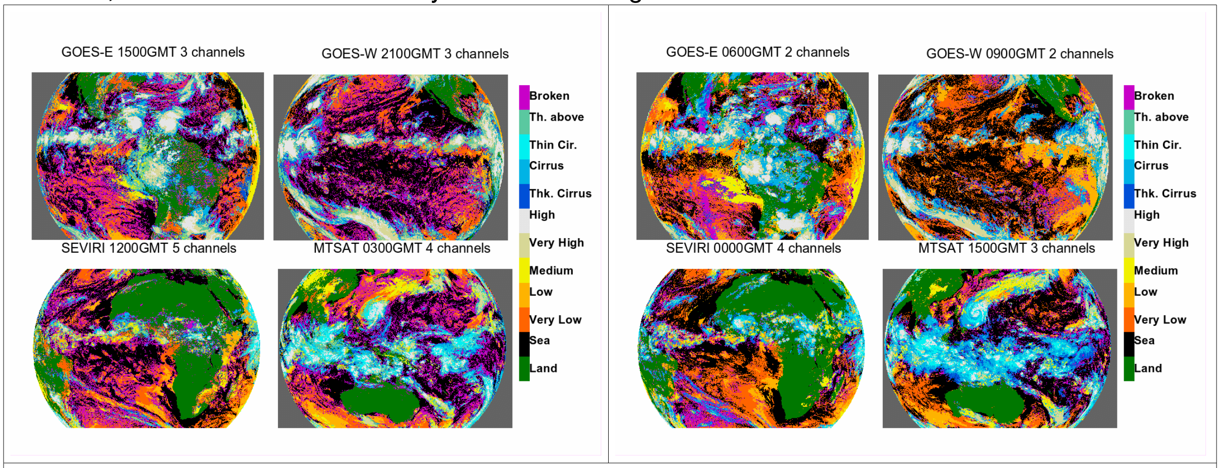

Figure 2: Example of Nigttime (left panel) and daytime (right panel) cloud type classification for GOES-E, GOES-W, SEVIRI and MTSAT obtained for GOES-E, GOES-W and MTSAT after a adaptation of the channels, the surface properties atlas.

3. EVALUATION OF THE SEVIRI CLOUD CLASSIFICATION BY COMPARISON AGAINST COLLOCATED SPACEBORNE LIDAR CLOUD TOP: THE DATA AND THE PERIODS

3.1 The GLAS and CALIOP lidar data

Space lidars provide unambiguous cloud top height (CTH) retrieval of the uppermost layer in nearly all situations and the CTH of the lower layers in case of upper optically thin (optical thickness <3) or broken dense layers. They are able to detect very small cumulus and thin cirrus (optical thickness down to about 0.01, McGill et al, 2007). However, thin cloud layer detection depends on the signal to noise ratio. Lidar signals are usually required to be averaged to increase signal-to noise ratio to better detect optically thin clouds. In the daytime data the SNR is small compared to nighttime data due to scattered sunlight. The cloud and aerosol CALIOP operational products (CALIPSO ATBD, 2005) are given at different scales (333m, 1, 5, 20 km)(Vaughan et al. 2004).

The lidar GLAS is on board the polar orbiter ICEsat platform launched in spring 2003. The lidar CALIOP is on board the polar orbiter CALIPSO platform flying in the A-train Constellation. Both lidar operate at two wave length (532nm and 1064nm). The lidar CALIOP delivers data from June 2006. The lidar GLAS operates only over short period during spring and during fall. The sensitivity of the 532nm channel has quickly decreased after fall 2003. Both lidar delivers observations along the satellite track. The laser beam diameters at surface are about 70m. Footprints are produce every 333m for CALIOP and 172m for GLAS. For CALIOP, the vertical resolution is 30m from the surface to 8.2km. For altitudes higher than 8.2km it is 60m (Winker et al. 2007). For GLAS, the vertical resolution is 76.8m (Palm et al. 2002; Spinhirne et al.2006). The cloud and aerosol CALIOP operational products (CALIPSO ATBD, 2005) are given at different scales (333m, 1, 5, 20 , 80 km)(Vaughan et al. 2004). The cloud and aerosol GLAS products are given at 1.4km, 7km and 21km.

In this study, the CALIOP operational Level 2 V2.01 cloud layer boundary product and the version 26 of the GLA11 cloud layer and optical thickness (OT) available at the French ICARE data centre with respectively 5km and 7km resolution along track(~ 70m across-track) comparable to the size of the SEVIRI pixels is used. With this resolution, an elevated 1km depth ice cloud should be detected by the CALIOP lidar provided its optical thickness is greater than 0.03 (daytime). For CALIOP, the 5km product includes also the layers detected using 20km or 80km average profils of backscattered signal labeled clear at the 5km resolution. In the following we will refer to CALIOP or CALIOP 5km for the cloud profils which do not include these layers and CALIOP 80km when these thin layers are included.

3.2 ISCCP METEOSAT-DX

In order to help to the evaluation of the SEVIRI cloud cover against lidar cloud cover, the ISCCP METEOSAT DX cloud cover is introduced in the comparison. This cloud cover obtained from METEOSAT data is available every three hours from the analysis of the infrared (nighttime and daytime) and visible (daytime) full resolution data (5km x 5km at sub-satellite point) sampled to 30km spacing (Rossow et Schiffer, 1999). The cloud identification is performed with a simple threshold technique with IR and VIS clear-sky values established from statistical analysis. For daytime data, both IR and VIS/IR cloud fractions are used in the comparison.

3.3 Period, region and data colocation

GLAS data analyzed belong to the October, 1 and November, 12, 2003 period (referred to as the laser-2a period, Dessler et al., 2006). During this period the 532 nm channel was at its uppermost sensitivity. The overpass time of the ICESAT platform was between 6:30 and 8:30 local time in the morning and in the evening. The CALIOP data analyzed belong to October 2006. The AQUA-train overpasses are close to 13:30 pm and 1:30 am equator crossing times.

For the GLAS october 2003 period, the SEVIRI data have been especially reprocessed by the SAFNWC with the version 1.2 of the algorithm. GLAS/CALIOP observations for 86/250 half-orbits have been matched to the SEVIRI observations under the ICESAT/CALIPSO track, choosing the closest in time and space. The 15' time sampling of the SEVIRI data set allows for a time lag of +-7.5' between the lidar observation and the corresponding SEVIRI pixel. The viewing angle has been limited to 48° in this analysis to reduce difference with nadir observations.

GLAS/CALIOP and ISCCP METEOSAT DX data have also been matched in the same way together over for the 86/250 GLAS/CALIOP half-orbits. However, in this case the maximum time lag between the two sets of observation is 1h30. The METEOSAT DX cloud cover is retrieved using METEOSAT-7 data for the October 2003 period and METEOSAT-8 (SEVIRI) for October 2006.

To be coherent with the ISCCP classification (Rossow et al, 1999), the SAFNWC cloud type classification has been corrected to ensure the separation at 440hPa and 680hPa levels between high and middle clouds and middle and low clouds.

4. RESULTS

4.1 SEVIRI, GLAS, CALIOP and METEOSAT DX cloud covers

Cloud cover fractions (CCF) over the observation area are reported in figure 3 and table 2. They are defined as the number of pixel flagged as cloudy over the total number of pixel. The maps of figure 1 have been built using a latitude-longitude grid of 5° by 5°. Then a 3x3 grid box smoothing operator has been applied.
In the three data set, the same features are observed: large cloud occurrence over ocean and in the ITCZ over land, small occurrence of clouds over the deserts. Moreover, the variations in these features between the October 2003 and the October 2006 period are similar: more clouds over west Africa in 2003, more clouds over south Africa in 2006, less clouds offshore Brazil coast in 2006. But the land/ocean contrast is stronger in the SEVIRI data set than in the GLAS, CALIOP and DX one's as shown by the average values corresponding to these geographical distributions and given in table 2 .

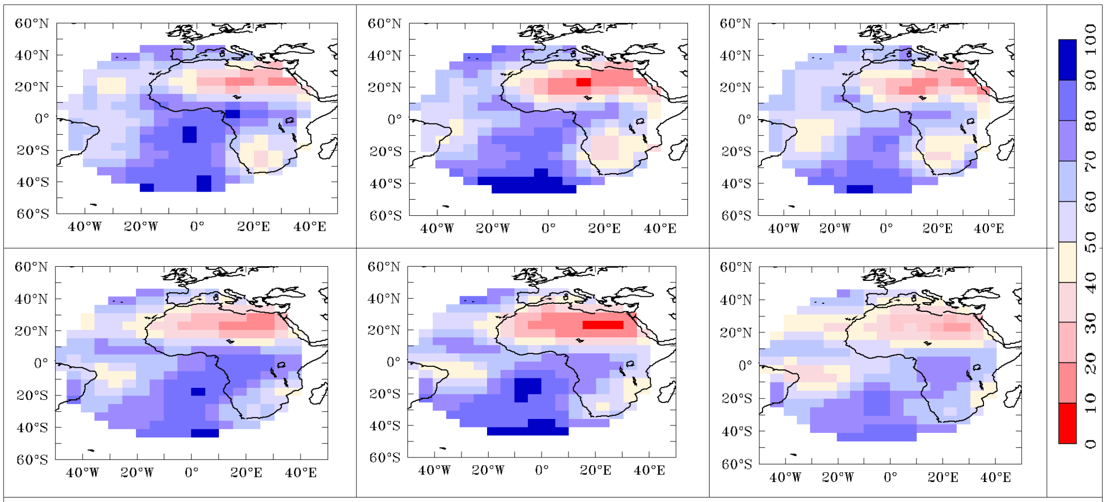

Figure 3: GLAS (left) , SEVIRI (center), DX (right) October 2003 mean cloud cover (top raw), CALIOP (left) , SEVIRI (center), DX (right) October 2006 mean cloud cover (bottom raw). For DX: day+nigh IR+VIS

In order to evaluate the contribution of very thin clouds not detectable with meteorological passive radiometer of spatial resolution larger than the kilometer, in table 2 for the lidar two CCF's are given. To compute these CCF's cloudy column with optical thickness smaller than an OT threshold value of respectively 0.02 or0.2 are not taken into account. In the following they will be called CCF-0.02 and CCF-0.2. Below 0.02 in OT the frequency of lidar cloudy column is smaller than 3% during nighttime and null during daytime.

	October 2003				October 2006					
	GLAS OT>0.02	GLAS OT>0.2	SEVIRI	ISCCP-MDX	CALIOP 5km OT>0.02	CALIOP 5km OT>0.2	SEVI.	ISCCP-MDX	CALIOP80km OT>0.02	CALIOP80km OT>0.2
Ocean Night	78	72	70	62	73	69	72	61	81	78
Ocean Day	68	62	76	63/69*	62	59	71	57/63*	79	76
Land Night	61	50	46	45	55	48	42	43	62	54
Land Day	50	39	40	42/48*	52	46	44	51/61*	65	58

Table 2: GLAS/SEVIRI /ISCCP and CALIOP/SEVIRI/ISCCP CCF observed over the selected area. For GLAS and CALIOP is given the fraction of cloudy column with OT larger than 0.02 and 0.2. For CALIOP, CALIOP 5km and CALIOP 80km CCF are given. ISCCP values are reported using IR only for nighttime, and IR/VIS channels for day time (numbers marked with *)

The lidar cloud cover is larger than SEVIRI cloud cover, excepted over ocean during day time. The mean lidar cloud cover after application of a threshold on OT of 0.2 is close from the SEVIRI one. The IR M-DX cloud cover is close from the SEVIRI one over land but there is a large underestimation over ocean. The sign and/or amplitude of the night to day cloud cover variations are not the same in the SEVIRI data set and in the lidar data set as well for midday-midnight October 2006 set than the evening-early morning October 2006 set. In all cases, from night to day the lidar CCF decreases. During daytime, the atmospheric background signal increases due to scattered sunlight. This make difficult the detection of thin layers. There is a large increase in CCF especially over ocean during daytime when the CALIOP 80km is used instead of CALIOP 5km. We notice that this is true as well for CCF with a 0.02 threshold value on OT than CCF with a 0.2 threshold value on OT.

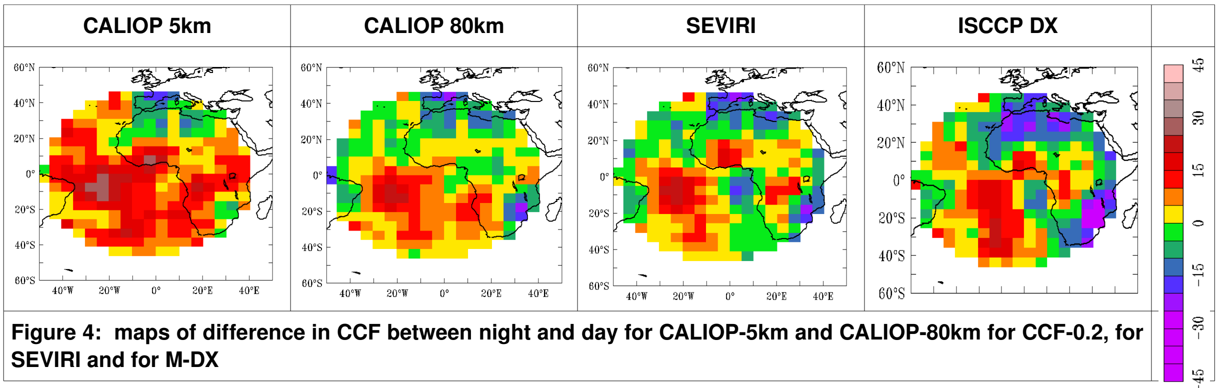

Figure 4: maps of difference in CCF between night and day for CALIOP-5km and CALIOP-80km for CCF-0.2, for SEVIRI and for M-DX

Figure 4 gives the maps of difference in CCF between night and day for CALIOP-5km and CALIOP-80km for CCF-0.2, for SEVIRI and for M-DX. For CALIOP-5km, the decrease in CCF observed for the mean CCF's in table 1 is verified for almost all the regions, excepted over south Europe and North Africa. The main structures in the night to day CCF variation maps for CALIOP-80km, SEVIRI and ISCCP M-DX are relatively similar. At 0130am compared to 0130pm, there is more clouds over south Atlantic, there is less clouds over south Europe and north Africa, there is less clouds over the Mozambique.

To go further in the analysis of the differences between SEVIRI and the lidar data sets, we have looked to coincident cloud or clear air detection at the pixel scale. The frequency of agreement or hite rate (HR) expressed as the sum of frequency of coincident cloud detection and clear detection by GLAS and SEVIRI and CALIOP and SEVIRI are similar. We notice that this was not the case for the differences between mean CCF's in table1. The HR is between 82% and 84% as well over ocean than over land, as well during day than during night and as well for GLAS than for CALIOP 5km data. Over land, the HR decreases by 7% when the CALIOP 80km data developed to detect very thin layers is used and on the contrary slightly increases (2%) when the 0.2 OD test is applied. Over ocean, if only homogeneous 3x3 pixel scene (all clear or all cloudy) are taken into account in the comparison which allows to reject pixels covered by broken clouds, the HR reaches 88%. In agreement with the mean cloud cover comparison, as well over ocean than land the frequency of SEVIRI cloudy pixels detect clear by the lidar is larger during day than during night and larger over ocean than over land. .

4.2 SEVIRI, GLAS, CALIOP cloud top pressure and cloud types

The cloud top pressure distributions for GLAS, CALIOP and SEVIRI are given in figure 5. The cloud top pressure distributions are built for each data set using all the pixels for which a pressure is available in this data set. These pixels can be or not clear in another data set. Each curve is normalized by the number of pixel used to built the distribution. In figure 5 is also given for SEVIRI, the frequency of partially covered pixels for which no pressure is available (blue line on the right of the figures). Is also given the frequency of high, midlevel and low cloud for the GLAS, CALIOP and SEVIRI.

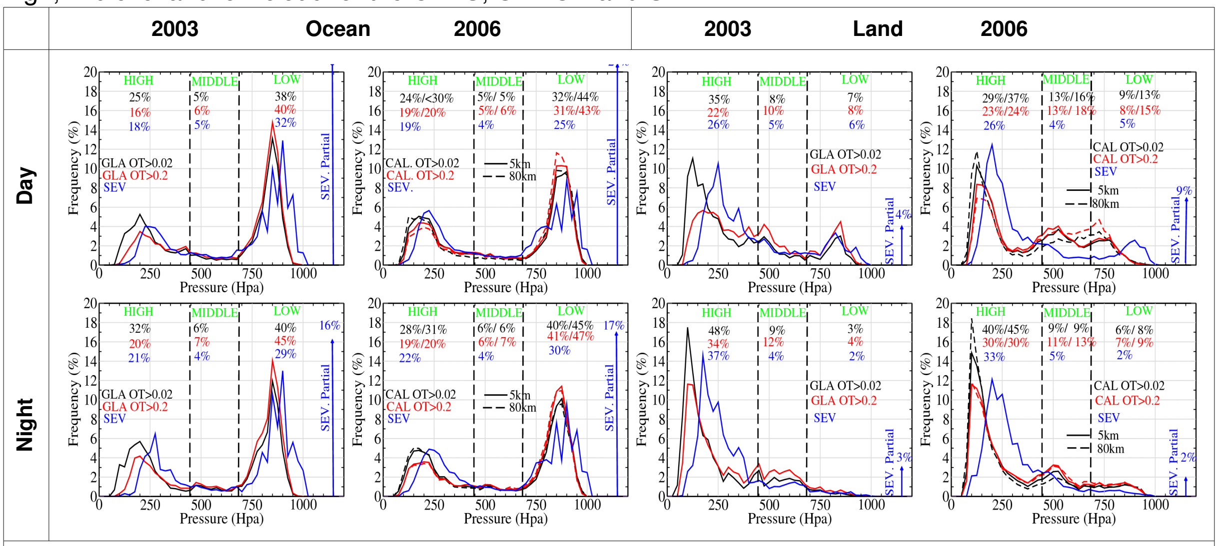

Figure 5: Cloud top pressure distribution for SEVIRI (blue curve), the lidar for an OT > 0.02 threshold (black curve), the lidar for an OT > 0.2 threshold (red curve) for ocean (left panel) and land (right panel) for day (top raw) and night (bottom raw) for GLAS and SEVIRI (left figures of the ocean and land panels), for CALIOP and SEVIRI (right figures of the ocean and land panels). For CALIOP both the CALIOP 5km (straight line) and CALIOP 80km(dotted line) are given.

The shapes of the lidar and SEVIRI cloud top pressure are very similar. Over ocean SEVIRI and CALIOP cloud top pressure have two well defined peaks at high and low pressure associated to the large occurrence of high clouds and low level clouds and small occurrence of mid-level cloud top.
Over land, the frequency of very high clouds is large and increases in the nighttime distributions. During daytime, low-midlevel cloud frequency increases. This is in agreement with the diurnal cycle of convection over land but it could be also due to the smaller SNR in the lidar daytime data. We notice that for October 2006, CALIOP and SEVIRI do not agree on the level of these midlevel-low clouds.

As well over ocean than over land, the SEVIRI high cloud top are not so high than the lidar cloud top. This is due to the larger sensitivity of the lidar instrument compare to passive radiometry to very small optical thickness/emissivity. Seze et al. (2008) have shown that the bias between the CALIOP and SEVIRI cloud top for very high clouds depends on the sounder channel used to estimate the SEVIRI cloud top pressure.

SEVIRI minus CALIOP				
	Low – Low (5km)	**Low+partial - Low (5km)**	**Low+part. - Low (80km)**	**Middle – Middle (80km)**

Day

Night

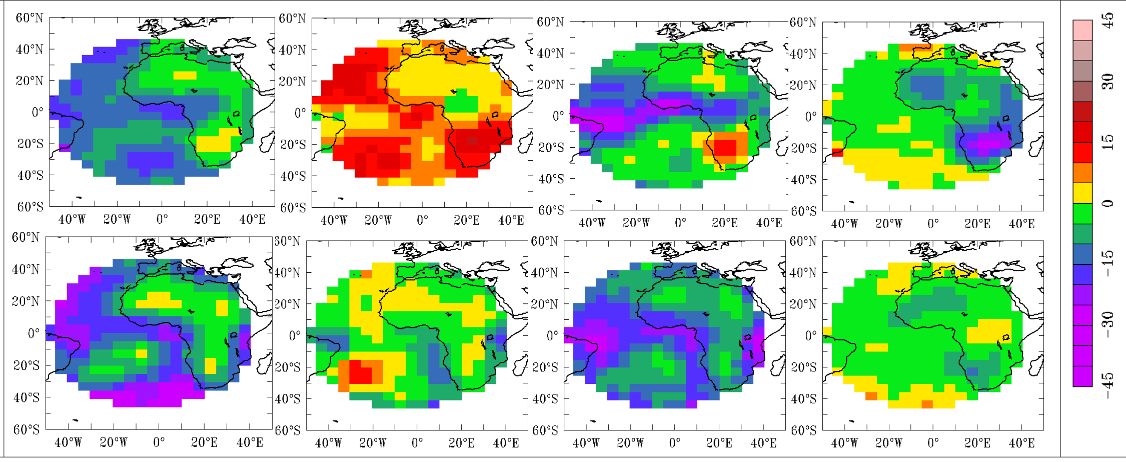

Figure 6 : SEVIRI minus CALIOP cloud fraction for low and middle level clouds for daytime data (first raw) and nighttime data (second raw)for the 0.02 OT threshold and the 5km and 80km resolution. For CALIOP, low cloud fraction is the sum of low cloud top fraction and low cloud under high or mid-level cloud fraction.

Over ocean, the fraction of SEVIRI pixels classified as partially covered is high, 16% during nighttime and more than 20% during day time. Figure 6 shows that if the SEVIRI and CALIOP-5km low cloud cover maps are compared, SEVIRI underestimates low cloud cover. This is no more the case if the partially covered pixels are added to the SEVIRI low clouds pixels. Now, during day time the overestimation of the low cloud cover by SEVIRI is above 10% in the oceanic regions well known for the high frequency of small cumulus. The increase in low cloud fraction is high when using CALIOP-80km instead of CALIOP-5km. In that case, SEVIRI misses a large amount of low clouds in the ITCZ where high clouds are very frequent. Over land, there is a striking feature in the SEVIRI minus CALIOP-80km maps above south Africa. The partially covered pixels must belong to mid-level clouds in this region in October 2006.

5. CONCLUSION

For the need of the MEGHA-TROPIQUES mission, the SAFNWC cloud detection, cloud classification and cloud top pressure algorithmes have been adapted to GOES-E, GOES-W, GOES-10, MTSAT, FY-2C.

As a first step to evaluate these cloud fields, SEVIRI cloud cover and cloud top pressure distributions have been compared with October 2003 GLAS data and October 2006 CALIOP data for land and ocean night and day data separately. The same behaviour of GLAS and CALIOP versus SEVIRI is found for the cloud cover. Excepted for daytime over ocean, the CCF obtained from 5km average lidar profils is larger than the SEVIRI cloud cover. Over land during nighttime, the underestimation of cloud cover by SEVIRI is large. Application of a threshold on OT of 0.2 in the lidar data reduces to 4% that underestimation.

The sign and/or amplitude of the night to day cloud cover variations are not the same in the SEVIRI data set and in the lidar data set as well for midday-midnight October 2006 set than the evening-early morning October 2006 set. In all cases, from night to day the lidar CCF decreases. During daytime, the atmospheric background signal increases due to scattered sunlight. This makes the detection of thin layers and perhaps of small broken clouds with 5km/7km average profils difficult as shown by the analysis of the SEVIRI and CALIOP low cloud cover frequency difference maps. To evaluate at least the sign of the cloud cover diurnal cycle, use of the CALIOP80km cloud cover seems to be more appropriate than the CALIOP-5km cloud cover. More investigation are required.

The shape of the CALIOP and SEVIRI cloud top pressure are close. As well over land than over ocean there is a peak at low pressure. Over ocean, there is another peak at high pressure. In the SEVIRI data set, the peak at low pressure is not so low than in the lidar data set due to the less sensitivity of the passive imager compared to the lidar. Over ocean, the peak at high pressure is relatively well positioned in the SEVIRI distribution but there is some too high cloud top pressure. This must be investigated. Over ocean, partially covered pixels are very frequent and not attributed to any specific level. These pixels are classified low clouds, low clouds under high clouds or clear by the lidar in 80% of the cases.

In the near futur, the same study will be performed with MTSAT, GOES-E, GOES-W and FY-2C.

REFERENCES

ATBD, Vaughan, M.A., D. M. Winker, K.A. Powell et al. (2005): Feature Detection and Layer Properties Algorithms – CALIOP PC-SCI-202 Part 2 Release 1.01 27 September 2005.

Derrien, M. and H. Le Gléau, 2005, MSG/SEVIRI cloud mask and type from SAFNWC. International Journal of Remote Sensing, 26, 4707-4732.

Derrien, M., H. Le Gléau, 2009: Improvement of cloud detection near sunrise and sunset by temporal-differencing and region-growing techniques with real-time SEVIRI. International Journal of Remote Sensing. (in press)

Menzel, W. P., W. L. Smith, and T. R. Stewart (1983): Improved cloud motion wind vector and altitude assignment using VAS. J. Appl. Meteorol., 22, 377-384.

Palm, S., W.Hart, D. Hlavka, E.J. Welton, A. Mahesh, and J. Spinhirne 2002: Geoscience Laser Altimeter System (GLAS) atmospheric data products, algorithm theoritical basis document, version 4.2, pp 137, NASA Goddard Space Flight Center, Greenbelt, Md.

Rossow, W.B., and R.A. Schiffer, 1999: Advances in understanding clouds from ISCCP. Bull. Amer. Meteorol. Soc., 80, 2261-2288, doi:10.1175/1520-0477(1999)

Schmetz, J., K. Holmlund, J. Hoffman, B. Strauss, B. Mason, V. Gaertner, A. Koch and L. van de Berg, (1993), Operational cloud motion winds from METEOSAT infrared images. J. Appl. Meteorol., 32, 1206-1225.

Sèze, G., F. Parol, C. Vanbauce, H. Le Gleau, M. Derrien, M. Lalande J. Riedi and J.C. Buriez: Comparison of SEVIRI cloud product with both the POLDER and the GLAS space lidar one. ESA SP-619., 37-42, Proc Third MSG workshop. Helsinki, 5 Juillet 2006.

Seze G., S. Marchand, J. Pelon and R. Borde, 2008: Comparison of AMV cloud top pressure derived from MSG with space based lidar observations (CALIPSO), 2008 EUMETSAT Meteorological Satellite Conference, Darmstatd, Germany, 8-12 September 2008.

Winker, D., W. Hunt, and M. McGill (2007), Initial performance assessment of CALIOP, Geophys. Res. Lett., 34, L19803, doi:10.1029/2007GL030135.

McGill, M. J., M. A. Vaughan, C. R. Trepte, W. D. Hart, D. L. Hlavka, D. M. Winker, and R. Kuehn (2007), Airborne validation of spatial properties measured by the CALIPSO lidar, J. Geophys. Res. , 112, D20201, doi:10.1029/2007JD008768

Scientific report an Additional Tuning of MSG PGE01-02-03 following validation activities. To be downloaded from www.meteorologie.eu.org/safnwc

User Manual for the PGE01-02-03 of the SAFNWC/MSG: Scientific Part. To be downloaded from www.meteorologie.eu.org/safnwc

Acknowledgements

The authors would like to thanks the NASA, CNES and ICARE data center for giving access to CALIOP data and GLAS data and the SATMOS and METEO-France for giving access to the geostationary data set.